JETIR.ORG ISSN: 2349-5162 | ESTD Year : 2014 | Monthly Issue
JOURNAL OF EMERGING TECHNOLOGIES AND INNOVATIVE RESEARCH (JETIR)
An International Scholarly Open Access, Peer-reviewed, Refereed Journal

PV ARRAY-BASED OFF-BOARD ELECTRIC VEHICLE BATTERY CHARGER

[1]P. Chaithanyakumar, [2]S. Ashok, [3]S. Nikhil, [4]M. Vikram, [5]G. Harish

[1, 2,3,4,5] Electrical and Electronics Engineering,
[1, 2,3,4,5] Gokula Krishna College of Engineering, India

Abstract: In the last ten years, the invention of electric vehicles (EVs) led to a boom in the industry of automobiles. The development of battery charging systems is crucial to the success of EVs. An electric vehicle's consumption of load rises when it is charged by the grid. This leads to the research's proposal of an off-board EV battery charging system based on photovoltaic (PV) arrays. The EV battery needs to be continuously charged irrespective of solar radiation, which can be achieved by using a backup battery bank in addition to the PV array. The suggested solution can charge the EV battery during both sunny and cloudy periods of the day by using the sepic converter and a three-phase bidirectional DC-DC converter. The backup battery helps to charge the EV battery during non-sunny hours, and also charges the EV battery simultaneously during peak sunshine hours. This study presents an overview of constructing and analyzing an experimental prototype in the laboratory and simulating the suggested charging system using Simulink in MATLAB software.

Introduction

Environmental issues arise from the ever-increasing consequences of greenhouse gasses from conventional internal combustion engines. This cleared the way for the automotive sector to see a rise in pollution-free electric vehicles (EVs)[1-3]. Alternative energy sources must be used because charging EV batteries from the utility grid makes a greater load on the grid and ultimately increases EV customers' electricity costs [4, 5]. Renewable energy sources (RESs) are infinite and emit no pollution, hence they can be utilized to recharge an electric vehicle's battery. Hence, "green transportation" refers to EVs powered by RES [6]. One of the most effective RESs that is readily available for use in EV battery charging is solar energy [7, 8]. In the suggested system, power converter topologies are utilized to enable the PV array electricity to be utilized for charging the EV battery.

The high-power density, high efficiency, low weight, and small size of lithium-ion batteries make them a popular choice for electric vehicles [9, 10]. Along with having a long lifespan and a low self-discharge rate, these batteries may also be charged quickly. Also, in the event of an overcharge or short circuit, they have a minimal chance of exploding. These batteries need careful voltage regulation while they're charging. Therefore, different voltage-controlled power electronic converters are employed to charge batteries in electric vehicles.

Power converters are required in order to charge the EV battery because of the PV array's periodic nature. Multiport converters (MPCs) are the converter of choice for hybrid electric vehicles (HEVs) onboard chargers because of their ability to interface energy storage components and power sources, such as photovoltaic arrays, ultra-capacitors, super capacitors, fuel cells, and batteries, with EV loads, such as motors, lights, power windows and doors, radios, amplifiers, and mobile phone chargers.

Because all of the sources are located within the EV, the MPCs have the disadvantage of increasing the weight, expense, and maintenance of the vehicle. Additionally, these converter-based EV battery charging systems become more advanced in terms of controller implementation. Therefore, an off-board charger is suggested in this study, where the PV array and backup battery bank are placed in the parking station or charging station, while the EV battery is kept inside the vehicle unit. The literature presents a variety of converter topologies for off-board charging systems.

Because it can operate in both boost and buck modes, the sepic converter is the recommended topology among several converter topologies. It also benefits from low input current ripple, reduced EMI, and the same input and output voltage polarity. However, in order to charge the EV battery during periods of poor solar irradiation and darkness, an additional storage battery bank is required. Depending on the amount of solar radiation, this backup battery bank must be charged in the forward direction and discharged in the reverse direction. As a result, a bidirectional converter that can handle both directions of power flow is needed.

There are two types of bidirectional converters: isolated and non-isolated converters. The isolation provided by the transformer in isolated converters raises the cost, mass, and dimensions of the converter. Because weight and size are EV's primary concerns, non-isolated bidirectional converters are the most appropriate for this use case.

The multiphase interconnection technique of the bidirectional interconnected DC–DC converter (BIDC) reduces ripple current and improves efficiency in discontinuous conduction mode, making it the preferred non-isolated bidirectional converter topology. It also has a minimal inductance value. By using zero voltage resonant soft switching, the turnoff losses are decreased by using a snubber capacitor across the switches. The parasitic ringing impact of the inducer current is also lessened. The additional benefits of this bidirectional converter are as follows.

The off-board EV battery charging system described in uses PV array electricity to charge the EV battery using a bidirectional DC–DC converter when the EV is in a standstill mode. When the EV is operating, the EV battery is discharged to power the vehicle's DC load. The disadvantage is that an EV battery can only be charged in the presence of sunlight. The suggested charger is designed using a PV array integrated with a sepic converter, a bidirectional DC–DC converter, and a backup battery bank to overcome this drawback and provide continuous EV battery charging.

Functionality of the proposed system

As seen in Fig. 1, the proposed PV-EV battery charger is composed of an EV battery, a backup battery bank, a controller, a sepic converter, a half-bridge BIDC, and a PV array. In order to get a consistent output voltage at the DC link, the controller generates the gate pulses that go to the sepic converter. Additionally, gate pulses are created to drive the BIDC switches in buck and boost modes, which charge the backup battery from the PV array. As seen in Fig. 1, the suggested PV-EV battery charger is composed of an EV battery, a backup battery bank, a controller, a sepic converter, a half-bridge BIDC, and a PV array. To produce a consistent output voltage at the DC link, the controller generates gate pulses that are sent to the sepic converter. In order

to run the BIDC in boost mode—which charges the backup battery from the PV array—and buck mode—which charges the EV battery from the backup battery—gate pulses to the BIDC switches are also created. The auxiliary switches Sa, Sb, and Sc receive gate pulses generated by the controller as well. Every auxiliary switch is turned on during periods of high solar radiation in order to interface the dc connection with the EV battery, the dc link with the backup battery through BIDC, and the dc link with the PV array through the sepic converter. The PV array and sepic converter are isolated from the DC link when switch Sa is switched OFF, indicating poor solar irradiation. In contrast, when there is not enough solar power to charge the backup battery, the switch Sc is switched OFF to disconnect the BIDC and backup battery from the DC connection. As this section explains, there are three modes in which the suggested system can function: mode 1, mode 2, and mode 3.

Mode 1

In order to charge the backup battery and EV battery simultaneously from the PV array through a separate converter and BIDC, respectively, all of the auxiliary switches are turned on during peak sunshine hours when the generated PV array power is higher. The backup battery is charged in this mode by the forward-operating BIDC, which raises the dc link voltage.

Mode 2

The output from the PV array is insufficient to charge an EV battery during periods of low solar irradiation and dark clouds. Switches Sa, SB, and Sc are thus turned OFF, disconnecting the PV array from the DC link, and connecting the EV battery to the backup battery via BIDC. BIDC steps down the backup battery voltage to charge the EV battery when operating in reverse direction in this mode.

Mode 3

Switches Sa and Sb are turned ON and switch Sc is turned OFF to disconnect the backup battery bank and BIDC from the DC link when the power provided by the PV array is sufficient to charge only the EV battery.

Design of the converters used in the proposed charger

SEPIC CONVERTER

The PI controller is used to modify the duty ratio of the sepic converter in the proposed charging system, ensuring a consistent output voltage regardless of the PV array voltage. As illustrated in Fig. 2, the components of the sepic converter are one IGBT switch, one diode, two inductors, and two capacitors. One of the main benefits of the sepic converter is that, in contrast to buck-boost and buck converters, it may function in both boost and buck modes based on the duty ratio [16]. Secondly, it produces an output voltage that is identical in polarity to the input voltage. Equation (1) provides the voltage gain of the sepic converter.

$$\frac{V_{dc}}{V_{PV}} = \frac{D}{1-D} \qquad (1)$$

where D is the sepic converter's duty ratio, VPV is the PV array voltage, and Vdc is the dc link voltage. The sepic converter's inductors and capacitors are selected based on (2)–(4) [17]:

$$L_a = L_b = \frac{V_{PVmin} D_{max}}{2\Delta i_{PV} f_{sw}} \quad (2)$$

$$C_1 = \frac{I_{dc} D_{max}}{\Delta V_{C1} f_{sw}} \quad (3)$$

$$C_2 = \frac{I_{dc} D_{max}}{\Delta V_{dc} f_{sw}} \quad (4)$$

Where fsw is the switching frequency, ΔVC1 is the capacitor, ΔVdc is the output voltage ripple, ΔVdc is the input current ripple, VPVmin is the minimum PV array voltage, and Dmax is the maximum duty ratio. These values are calculated as follows:

$$D_{max} = \frac{V_{dc} + V_D}{V_{PVmin} + V_{dc} + V_D} \quad (5)$$

where the diode voltage drop is represented by VD.

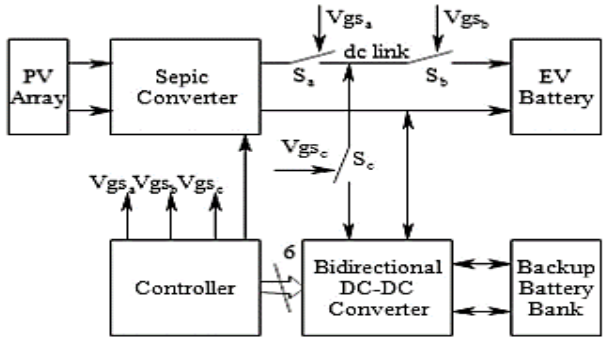

fig 1, electric vehicle battery charger block diagram

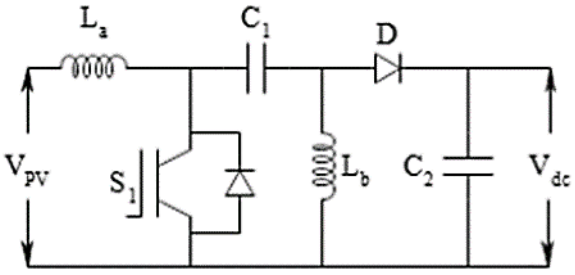

fig 2, diagram schematic for the sepic converter

Bidirectional interleaved DC–DC converter

The schematic diagram of the BIDC used in the suggested charging method is shown in Fig. 3. The converter's dc link is on the low voltage side, while the backup battery bank is on the high voltage side. This converter operates in two modes: buck mode in reverse and boost mode in forward motion. The active switches in boost mode are switches SL1, SL2, and SL3, and the active switches in buck mode are switches SU1, SU2, and SU3. Every switch used in this converter has a parallel snubber capacitor and an antiparallel diode. The inductors L1, L2, and L3 function as boost inductors in boost mode and as a low-pass filter in buck mode, respectively. The components of this converter's smoothing energy buffer are the capacitors, CL, and CH. The current ripples are reduced by interleaved inductor currents. Analyzing the converter's modes of operation involves taking a look at how a single-leg converter functions in [20]. In both the boost and buck modes, the voltage conversion ratio of the BIDC is provided as below.

$$\frac{V_{BackupBatt}}{V_{dc}} = \frac{1}{1-D_{Boost}} \quad (6)$$

$$\frac{V_{dc}}{V_{BackupBatt}} = D_{Buck} \quad (7)$$

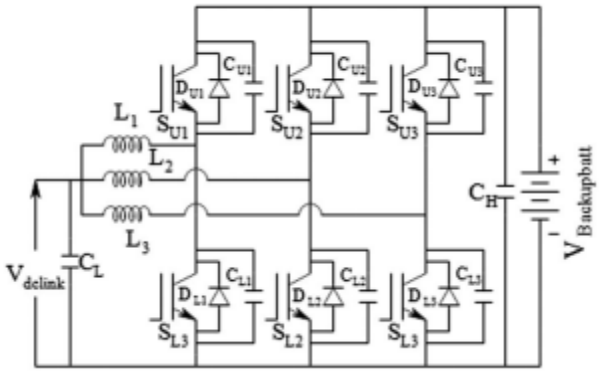

fig. 3: half-bridge bidc schematic diagram

Where D Boost is the BIDC duty ratio in boost mode, D Buck is the buck mode duty ratio, and V Backup Batt is the backup battery voltage. In order to operate the converter in discontinuous conduction mode and increase efficiency, the values of the inductors are thought to be less than the critical inductance values in both the boost and buck modes [20]. The following equations are used to compute the critical inductance value in the boost and buck modes.

$$L_{cric} = \frac{3V_{Backup}^2 D_{Boost}(1-D_{Boost})^2}{2Pf_s} \quad (8)$$

$$L_{cric} = \frac{3V_{dc}^2(1-D_{Buck})}{2Pf_s} \quad (9)$$

where P is the power from the backup battery. Based on the following formulae, the values of the capacitors on the high and low voltage sides of the BIDC are determined:

$$C_H = \frac{D_{Boost}P}{2f_s V_{BackupBatt}^2} \quad (10)$$

$$C_L = \frac{V_{BackupBatt} D_{Buck} (1 - D_{Buck})}{8 f_s^2 L \Delta V_{dc}} \quad (11)$$

Design of controllers

The proposed charger's controller produces gate pulses that are applied to the three auxiliary switches, the BIDC, and the sepic converter's switches. Fig. 4 shows the algorithm for turning the auxiliary switches ON and OFF. The controller calculates the PV array power after detecting the voltage and current of the array. In the event that the power generated by the PV array exceeds the rated power of the EV battery, or PR, the controller will create gate pulses that will activate all of the auxiliary switches, allowing the EV battery and backup battery bank to be charged simultaneously from the PV array. The switch, Sc, is turned OFF to disconnect the backup battery from the charging system and switches, Sa and Sb are turned ON to charge the EV battery alone from the PV array if the PV array power is less than the rated power of the EV battery but greater than the minimum required power. The switch, Sa, is switched OFF to isolate the PV array and split converter from the charging system if the PV array power is less than the minimum required power, PM. The backup battery may now charge the EV battery because the switches Sb and Sc are switched ON. In the suggested charging system, the PI voltage controller produces gate pulses to the MOSFET in the sepic converter to keep the voltage at the dc link constant regardless of changes in the PV array voltage.

BIDC is made up of three legs, each containing two switches. The two switches in the same leg must receive gate pulses that are 180 degrees apart in phase. Depending on the power of the PV array, the controller in the suggested system generates six gate pulses to the BIDC. Gate pulses are generated to the BIDC switches to run it in boost mode, increasing the dc link voltage to charge the backup battery bank, if PV array power exceeds PR. The leg 1 switches in this mode receive gate pulses with a 0° phase shift, the leg 2 switches receive a 120° phase shift from the leg 1 switches, and the leg 3 switches receive a 240° phase shift from the leg 1 switches. The gate pulses are generated to operate the BIDC in buck mode if the PV array power is less than PM. This produces a step-down voltage at the dc link that is adequate to charge the EV battery by using the backup battery. In this mode, leg 3 switches receive gate pulses with a 0° phase shift, whereas leg 2 and leg 1 switches receive gate pulses that are 120° and 240° phase displaced relative to the leg 3 switches, respectively.

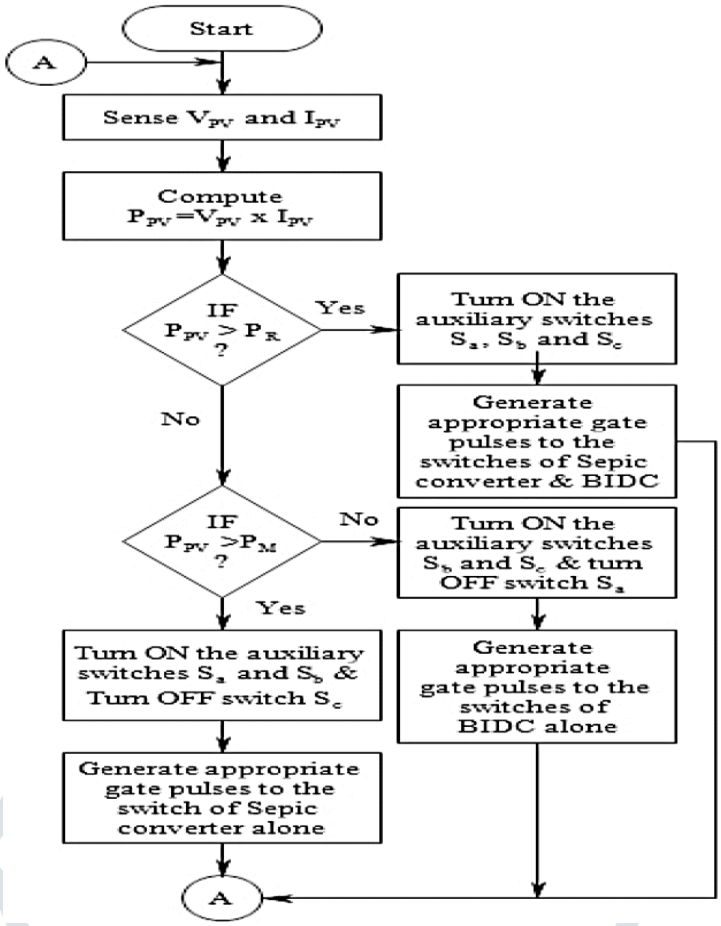

fig 4: flowchart for generating gate pulses for auxiliary switches

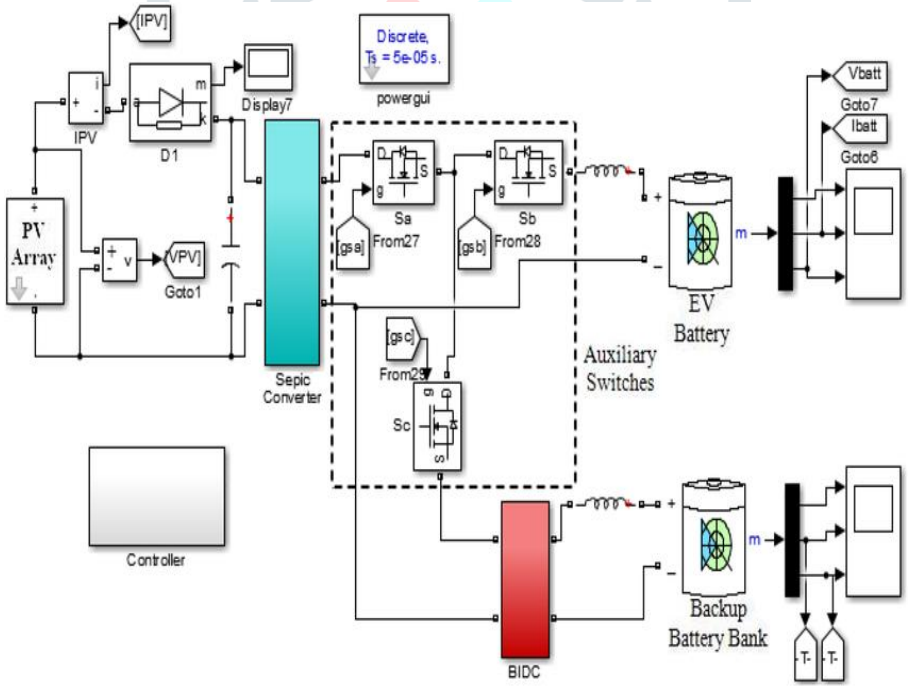

fig 5: a device simulation of the proposed charger

Mathematical modeling of proposed system

By integrating the state-space average model of the Sepic converter and the bidirectional DC-DC converter, the mathematical model of the suggested system is produced. It is calculated by taking the converters' ON and OFF switching periods into account. Req is the equivalent impedance at the dc link, and Ds is the duty ratio of the Sepic converter. These are the state space matrices of the Sepic converter, state matrix "A," input matrix "B," output matrix "C," and feed forward matrix "D."

$$A = \begin{bmatrix} 0 & 0 & \frac{-(1-D_s)}{L_a} & \frac{-(1-D_s)}{L_a} \\ 0 & 0 & \frac{D_s}{L_b} & \frac{-(1-D_s)}{L_b} \\ \frac{(1-D_s)}{C_1} & \frac{-D_s}{C_1} & 0 & 0 \\ \frac{(1-D_s)}{C_2} & \frac{(1-D_s)}{C_2} & 0 & \frac{-1}{C_2 R_{eq}} \end{bmatrix}$$

$$B = \begin{bmatrix} \frac{1}{L_a} \\ 0 \\ 0 \\ 0 \end{bmatrix}$$

$$C = [0 \quad 0 \quad 0 \quad 1]$$

$$D = [0]$$

$$A_1 = \begin{bmatrix} \frac{-(R_{lp}+R_{dson})}{L} & 0 & \frac{-(1-D_{BIDC})}{L} \\ \frac{-1+2D_{BIDC}}{C_L} & 0 & 0 \\ \frac{(1-D_{BIDC})}{C_H} & 0 & \frac{-1}{C_H R_{eq1}} \end{bmatrix}$$

$$B_1 = \begin{bmatrix} \frac{1}{L} \\ 0 \\ 0 \end{bmatrix}$$

$$C_1 = [0 \quad 0 \quad 1]$$

$$D_1 = [0]$$

Similarly, it finds out that the state-space matrices of the BIDC, state matrix "A1," input matrix "B1," output matrix "C1," and feed forward matrix "D1" are where L = (L1/3), Rlp = (RL1/3), Req1 is the equivalent impedance across capacitor CH, Rdson is the MOSFET turn on resistance, RL1 is the inductor's parasitic resistance, L1 and DBIDC is the BIDC's duty ratio.

The overall transfer function of the proposed system is created by combining the transfer functions of the converters, which are calculated from the state-space models mentioned above. The suggested system is stable

as evidenced by the frequency response, which also shows favorable gain and phase margins. The proposed charger is the subject of simulation experiments, the results that are provided in the section that follows.

Simulation research and outcomes

The simulation studies of the proposed system are conducted using Simulink in the MATLAB software. The common equation for PV arrays is used to model them [28, 29]. Using power MOSFETs, inductors, and capacitors from the Sim Power Systems Block set in the Simulink library, the Sepic and BIDC converter is simulated.

The Simulink library's PWM generator, pulse generator, logic gates, comparator, multiplier, and PI controller are used to create the controller.

As seen in Fig. 5, the PV array model is combined with the constructed BIDC and sepic converter in addition to the battery models that are accessible in the Simulink library to construct the suggested charging system.

Figs. 6a and b, respectively, exhibit the constructed simulation model of the BIDC and sepic converter, which are shown as subsystems in Fig. 5.

Using the created simulation model for PV array irradiation of 850, 100, and 500 W/m2 in modes 1, 2, and 3, respectively, the dynamic response of the system was examined. Fig. 7 displays the simulation results, which include the gate pulses to the auxiliary switches as well as the PV array voltage and current waveforms. In Fig. 7, radiation waveforms at 1000 W/m2 are displayed on a scale of 1.

Therefore, in this mode, the backup battery and the EV battery are charged simultaneously. In contrast, the PV array power is insufficient to charge the EV battery at low sunlight levels of 100 W/m2, resulting in strong gate pulses for the auxiliary switches, Vgsb and Vgsc, and low gate pulses for Vgsa. The EV battery is charged in this mode by the backup battery bank draining through BIDC.

The backup battery is disconnected from the system when the auxiliary switches Sa, SB, and Sc are turned OFF during a 500 W/m2 radiation level. The backup battery is segregated and not charged in this mode since the power from the PV array is only enough to charge the EV battery. Given that the EV battery is continuously charged in all three modes, Fig. 7 illustrates that the gate pulses to the switch Sb are always high. When the electric battery is fully charged, turn off the switch, SB, to prevent the electric battery from trickling charge. The simulated dynamic waveforms for the PV array, EV battery, dc link, and backup battery at the appropriate radiation values are shown in Fig. 8. As seen in Figs. 8a and b, in mode 1, the PV array voltage, VPV of 33.3 V, is stepped down to the dc link voltage, Vdc of 28 V by sepic converter. This way of charging is indicated by an increase in the EV battery's state of charge (SOC) and its negative current, as shown in Fig. 8c. As shown in Fig. 8d, BIDC works as a boost converter in the forward direction in this mode, increasing the dc link voltage, Vdc, from 28 to 60.6 V to charge the backup battery with the rise in SOC.

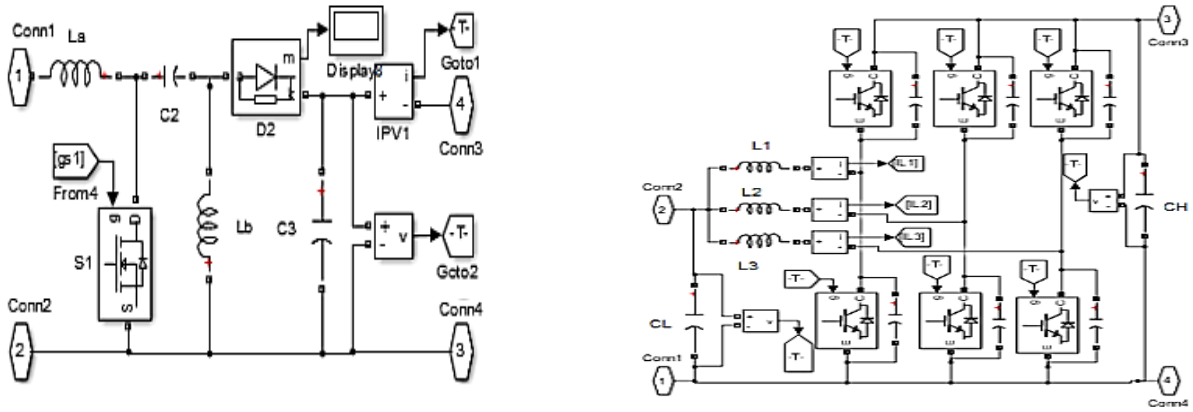

(a) (b)

fig. 6: simulation model of (a) sepic converter, (b) bidc

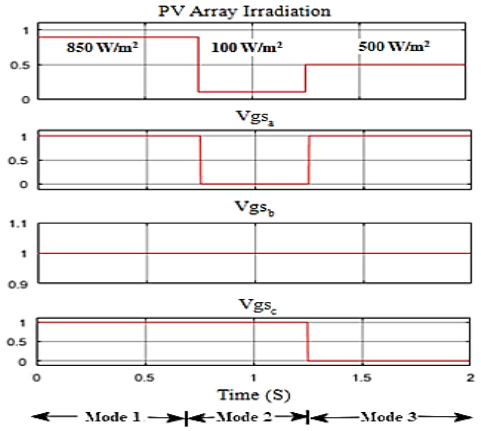

fig. 7 shows the gate pulses to the auxiliary switches and the waveforms of the pv array's radiation.

PV array voltage and current waveforms are shown in Fig. 8a. In mode 2 (during non-sunny hours and low irradiation circumstances), the PV array is isolated, resulting in PV array voltage, VPV, rising to its open circuit voltage of 37.25 V and PV array current, IPV, of 0 A. In order to charge the EV battery during this time, BIDC steps down the backup battery voltage to 27.32 V while operating in reverse buck mode, shown in Fig. 8c. As can be observed in Fig. 8d, the backup battery has been drained in this mode based on the positive current and drop in SOC. As observed in Fig. 8d, the backup battery voltage decreases to 55.2 V at the conclusion of this mode from 60.6 V. As seen in Figs. 8a and b, the PV array voltage, VPV of 31.81 V, is stepped down to a dc link voltage, Vdc of 27.6 V, in mode 3 in order to charge the EV battery. The EV battery is charging in this mode as well, as seen by the rising SOC and negative current. As illustrated in Fig. 8d, in mode 3, the backup battery voltage is kept at its prior value of 55.2 V and the current is lowered to zero since it is isolated from the charging system. In all three modes, Fig. 8c displays a negative current and growing state of charge (SOC) for the EV battery, indicating that it receives continuous charging from either the backup battery or the PV array.

In Fig. 9, the overlapped inductor current waveforms of the BIDC in all operating modes are displayed. Mode 2's reversal of the inductor current flow makes it visible that the backup battery is being drained, while

Mode 3's zero inductor current indicates that the BIDC is not connected to the charger. In order to provide validation for the simulation studies, a hardware prototype is created and tested; the outcomes are presented in the next section.

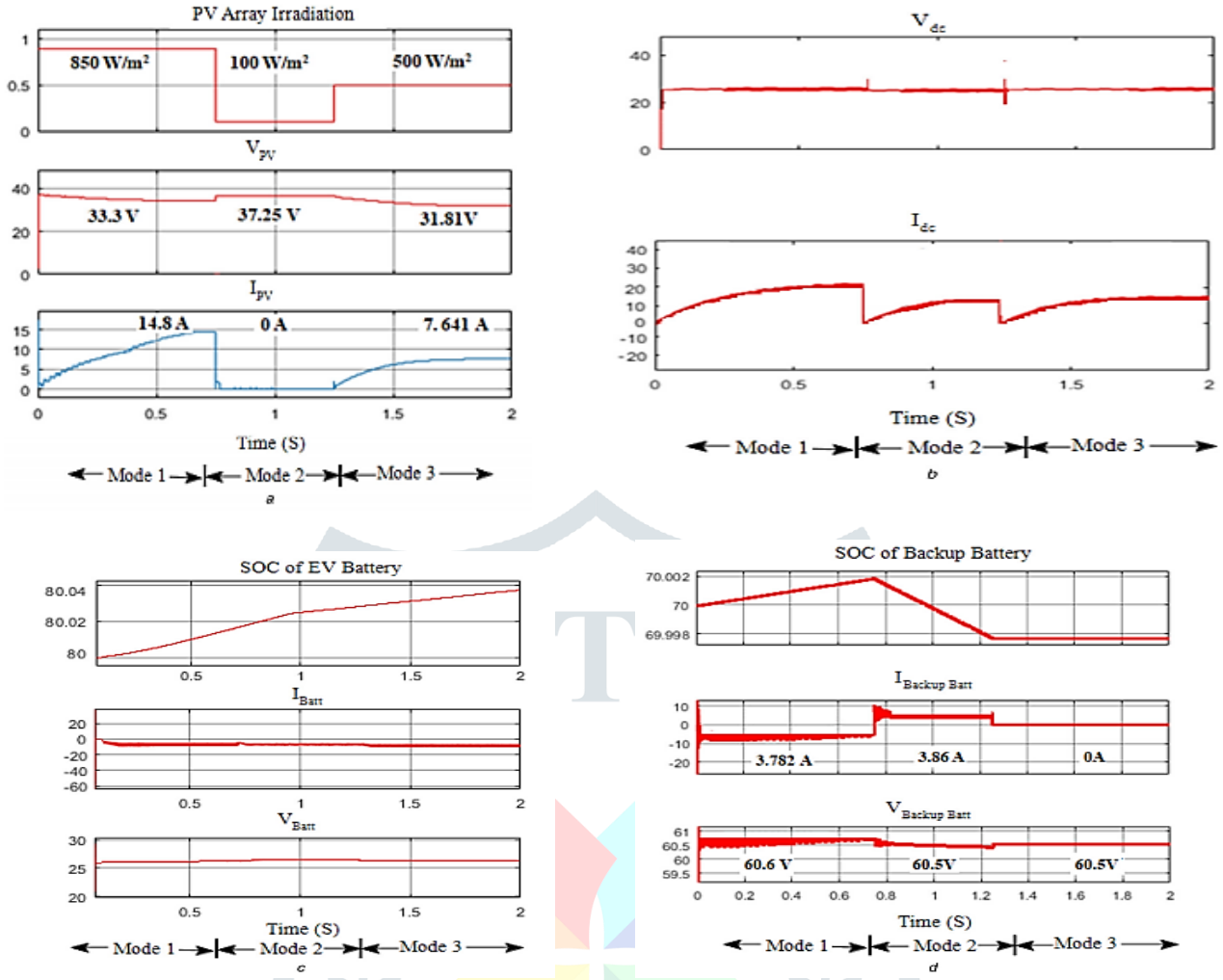

fig. 8 waveforms of (a) PV array voltage, v_{pv} & PV array current, I_{pv}, (b) dc link voltage, vdc, & current, I_{dc}, (c) EV battery soc, EV battery current, I_{batt}& EV battery voltage, V_{batt}, (d) backup battery soc, backup battery current, I_{backup} batt & backup battery voltage, V_{backup} batt

Conclusion

This research proposes an off-board photovoltaic array-fed off-board electric vehicle battery charging system. The ability of the system to continuously charge the EV battery regardless of the irradiation circumstances is covered in this study. The MATLAB Simulink environment is used to design and simulate the system. The three distinct modes of operation of the proposed charging system are tested individually on the hardware prototype in a laboratory setting, and the findings are reported. The OPAL-RT Real-time Simulator OP4500 is utilized for experimental inquiry using the RCP approach. The system's dynamic reaction is provided in both simulation and experimental investigation. The trial results and modeling results match well, highlighting the usefulness of the suggested charger.

References

[1] Santhosh, T.K., Govindaraju, C.: 'Dual input dual output power converter with one-step-ahead control for hybrid electric vehicle applications', IET Electr. Syst. Transp., 2017, 7, (3), pp. 190–200

[2] Shukla, A., Verma, K., Kumar, R.: 'Voltage-dependent modelling of fast charging electric vehicle load considering battery characteristics', IET Electr. Syst. Transp., 2018, 8, (4), pp. 221–230

[3] Wirasingha, S.G., Emadi, A.: 'Pihef: plug-in hybrid electric factor', IEEE Trans. Veh. Technol., 2011, 60, pp. 1279–1284

[4] Kirthiga, S., Jothi Swaroopan, N.M.: 'Highly reliable inverter topology with a novel soft computing technique to eliminate leakage current in grid-connected transformerless photovoltaic systems', Comput. Electr. Eng., 2018, 68, pp. 192–203

[5] Badawy, M.O., Sozer, Y.: 'Power flow management of a grid tied PV-battery system for electric vehicles charging', IEEE Trans. Ind. Appl., 2017, 53, pp. 1347–1357

[6] Van Der Meer, D., Chandra Mouli, G.R., Morales-Espana Mouli, G., et al.: 'Energy management system with PV power forecast to optimally charge EVs at the workplace', IEEE Trans. Ind. Inf., 2018, 14, pp. 311–320

[7] Xavier, L.S., Cupertino, A.F., Pereira, H.A.: 'Ancillary services provided by photovoltaic inverters: single and three phase control strategies', Comput. Electr. Eng., 2018, 70, pp. 102–121

[8] Krithiga, S., Ammasai Gounden, N.: 'Investigations of an improved PV system topology using multilevel boost converter and line commutated inverter with solutions to grid issues', Simul. Model. Pract. Theory, 2014, 42, pp. 147–159

[9] Sujitha, N., Krithiga, S.: 'RES based EV battery charging system: a review', Renew. Sustain. Energy Rev., 2017, 75, pp. 978–988

[10] Farzin, H., Fotuhi-Firuzabad, M., Moeini-Aghtaie, M.: 'A practical scheme to involve degradation cost of lithium-ion batteries in vehicle-to-grid applications', IEEE Trans. Sustain. Energy, 2016, 7, pp. 1730–1738